Journal of Asian Earth Sciences 127 (2016) 246–256

Contents lists available at ScienceDirect

Journal of Asian Earth Sciences

journal homepage: www.elsevier.com/locate/jseaes

Full length Article

Water geochemistry of the Qiantangjiang River, East China: Chemical weathering and CO_2 consumption in a basin affected by severe acid deposition

Wenjing Liu [a,b], Chao Shi [a,c], Zhifang Xu [a,*], Tong Zhao [a,c], Hao Jiang [a,c], Chongshan Liang [d], Xuan Zhang [a,c], Li Zhou [a,c], Chong Yu [a,c]

[a] Key Laboratory of Shale Gas and Geoengineering, Institute of Geology and Geophysics, Chinese Academy of Sciences, Beijing 100029, China
[b] Earth and Environmental Systems Institute and the Department of Geosciences, The Pennsylvania State University, University Park, PA 16802, USA
[c] University of Chinese Academy of Sciences, Beijing 100049, China
[d] State Key Laboratory of Environmental Geochemistry, Institute of Geochemistry, Chinese Academy of Sciences, Guiyang, Guizhou 550002, China

ARTICLE INFO

Article history:
Received 7 March 2016
Received in revised form 12 June 2016
Accepted 13 June 2016
Available online 15 June 2016

Keywords:
Qiantangjiang River
Chemical weathering
CO_2 consumption
Sulfuric acid

ABSTRACT

The chemical composition of the Qiantangjiang River, the largest river in Zhejiang province in eastern China, was measured to understand the chemical weathering of rocks and the associated CO_2 consumption and anthropogenic influences within a silicate-dominated river basin. The average total dissolved solids (TDS, 113 mg l^{-1}) and total cation concentration (TZ+, 1357 μeq l^{-1}) of the river waters are comparable with those of global major rivers. Ca^{2+} and HCO_3^- followed by Na^{2+} and SO_4^{2-}, dominate the ionic composition of the river water. There are four major reservoirs (carbonates, silicates, atmospheric and anthropogenic inputs) contributing to the total dissolved load of the investigated rivers. The dissolved loads of the rivers are dominated by both carbonate and silicate weathering, which together account for about 76.3% of the total cationic load origin. The cationic chemical weathering rates of silicate and carbonate for the Qiantangjiang basin are estimated to be approximately 4.9 ton km^{-2} a^{-1} and 13.9 ton km^{-2} a^{-1}, respectively. The calculated CO_2 consumption rates with the assumption that all the protons involved in the weathering reaction are provided by carbonic acid are 369×10^3 mol km^{-2} a^{-1} and 273×10^3 mol km^{-2} a^{-1} by carbonate and silicate weathering, respectively. As one of the most severe impacted area by acid rain in China, H_2SO_4 from acid precipitation is also an important proton donor in weathering reactions. When H_2SO_4 is considered, the CO_2 consumption rates for the river basin are estimated at 286×10^3 mol km^{-2} a^{-1} for carbonate weathering and 211×10^3 mol km^{-2} a^{-1} for silicate weathering, respectively. The results highlight that the drawdown effect of CO_2 consumption by carbonate and silicate weathering can be largely overestimated if the role of sulfuric acid is ignored, especially in the area heavily impacted by acid deposition like Qiantangjiang basin. The actual CO_2 consumption rates (after sulfuric acid weathering effect deduction) is only about 77% of the value calculated with the assumption that carbonic acid donates all the protons involved in the weathering reaction.

1. Introduction

Chemical weathering of rocks is a key process that links geochemical cycling of solid earth to the atmosphere and the ocean. It provides nutrients to terrestrial and marine ecosystems and regulates the level of atmospheric CO_2. To estimate chemical weathering rates and clarify the controlling factors on weathering rate is an important issue related to long-term global climate change because chemical weathering of silicate minerals is the net sink of atmospheric CO_2 over geologic timescales by consuming atmospheric CO_2 and subsequently storing it as carbonate sediments in the ocean (Négrel et al., 1993; Berner and Caldeira, 1997; Gaillardet et al., 1999; Kump et al., 2000; Amiotte-Suchet et al., 2003; Oliva et al., 2003; Hartmann et al., 2009; Moon et al., 2014). Therefore, many studies have used chemical discharge of rivers to estimate catchment and global chemical weathering rates and to examine the factors that control those rates, such as lithology, soil cover, vegetation, climate (temperature and precipitation), and relief (e.g., Raymo and Ruddiman, 1992; Gislason et al., 1996; Galy and France-Lanord, 1999; Huh, 2003; Millot et al., 2002, 2003; Oliva et al., 2003; Riebe et al., 2003; West et al.,

* Corresponding author.
E-mail address: zfxu@mail.iggcas.ac.cn (Z. Xu).

http://dx.doi.org/10.1016/j.jseaes.2016.06.010
1367-9120/

2005; Moon et al., 2007; Noh et al., 2009; Shin et al., 2011; Calmels et al., 2011; Goudie and Viles, 2012). However, with increasing influence of human activity, the potential for anthropogenic disturbance to natural chemical weathering processes should not be ignored (Roy et al., 1999; Raymond and Cole, 2003; Li et al., 2008; Chetelat et al., 2008; Pacheco et al., 2013). More and more studies focus on the anthropogenic sourced proton (e.g., released by sulfur mineral oxidation in mining areas or by N-fertilizer nitrification in agricultural catchments) impacts on chemical weathering (Galy and France-Lanord, 1999; Semhi et al., 2000; Spence and Telmer, 2005; Xu and Liu, 2007; Perrin et al., 2008; Gandois et al., 2011). Moreover, the role of acid deposition (mainly sulfuric acid) on these processes has also been investigated in some river basins (Amiotte-Suchet et al., 1995; Probst et al., 2000; Vries et al., 2003; Lerman et al., 2007; Xu and Liu, 2010). Amiotte-Suchet et al. (1995) estimated that acid rain decreased the atmospheric/soil CO_2 consumption by weathering by 73% in a small catchment located in the Vosges Mountains (north-eastern France). On a global scale, it would represent approximately 13% when considering sulfuric acid deposition (Amiotte-Suchet et al., 1995; Lerman et al., 2007; Perrin et al., 2008). The enhanced rock weathering by anthropogenic acid inputs must be considered as the modifications in weathering rates will influence the element fluxes to riverine systems and thus the carbon cycle.

Zhejiang, an eastern coastal province of China, is one of the most economically developed areas in China and has a population larger than 50 million. Moreover, it is also the most serious acid deposition affected area in the country (Fig. 1). The rainwater there is typically acidic with a volume-weighted mean pH of 4.54 (Zhang et al., 2007). In this study, the largest river (Qiantangjiang River) basin in Zhejiang province was first investigated, in order to estimate chemical weathering rates and examine the controlling factors on weathering rate. The goals of this study are: (i) to decipher the different sources of solutes and to quantify the contributions of the sources to the dissolved load; (ii) to calculate silicate and carbonate weathering rates and associated CO_2 consumption; (iii) to evaluate the effects of acid deposition on rock weathering in one of the most severe acid rain basin in China.

2. Study area

The Qiantangjiang River originates from Xiuning County at the north border of Zhejiang province in eastern China, lying between 28°10′ and 30°48′N latitude and between 117°37′ and 121°52′E longitude. It is the largest river in Zhejiang province with a length of 589 km and a drainage basin area of 55,600 km^2. The Xin'anjiang River and Lanjiang River converge at Meicheng and comprise the upper reaches of the Qiantangjiang River. The middle reaches are form Meicheng to Hangzhou city, and is also named Fuchunjiang River. The Qiantangjiang River finally flows into the East China Sea through the Gulf of Hangzhou (Fig. 1).

The Qiangtangjiang basin is in a subtropical monsoon climate regime with average annual temperature of 16.2–17.7 °C. The precipitation and runoff undergo significant intra-annual and inter-annually fluctuations. Average annual precipitation is between 1100 and 2400 mm, of which about 50% occurs between April and June, while 20% occurs from July to September. Due to the diversities of topography, the rainfall is unevenly distributed over

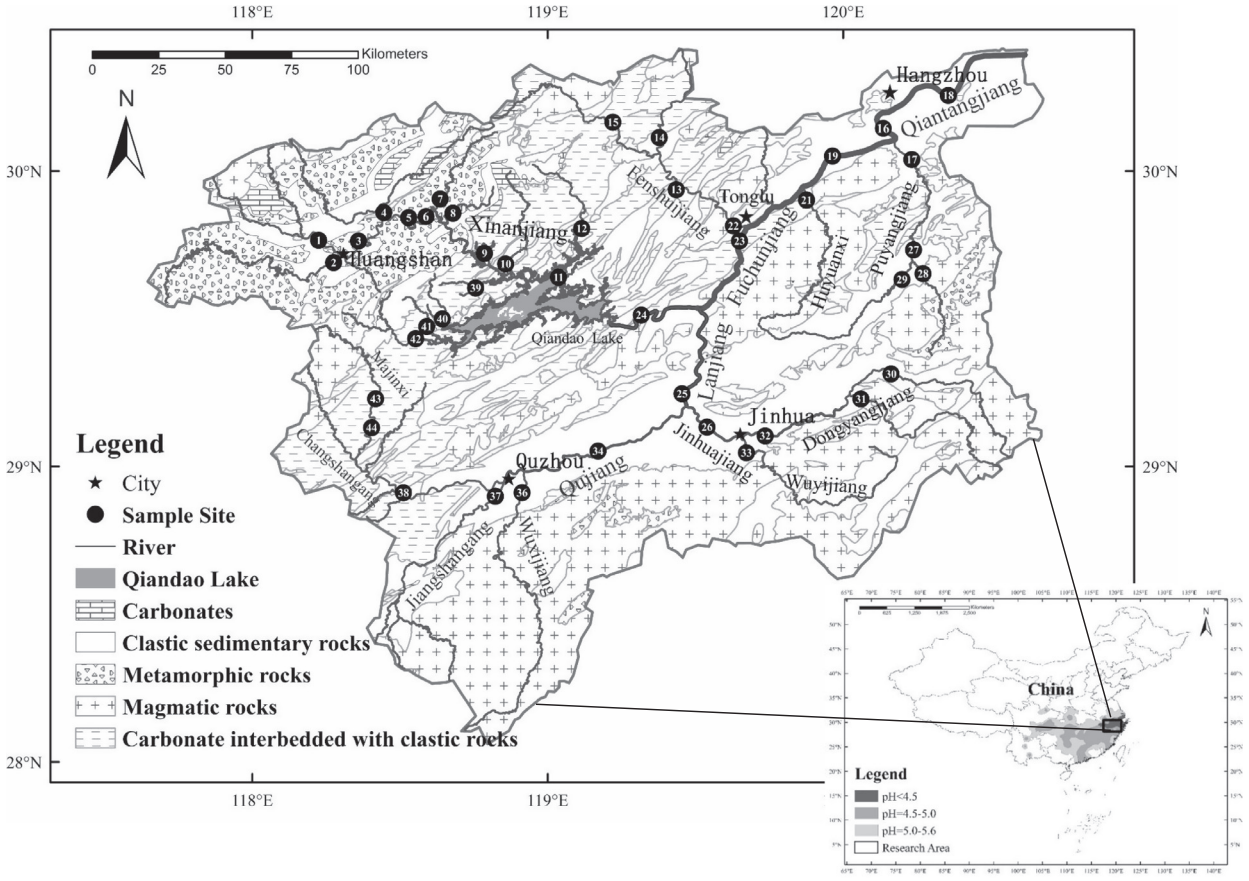

Fig. 1. Sketch map showing the lithology, sampling locations, and sample number of the Qiantangjiang River drainage basin, and regional rain water pH ranges are shown in the sketch map at the right bottom.

the entire basin with a general decline trend from southwest to northeast. Vegetation covers approximately 60.5% of the basin, with higher vegetation covering in upper reaches. Cultivated land, representing about 23.5% of the drainage area, is mainly located along the river networks, and industry and cities are mainly concentrated in the coastal areas such as Hangzhou and Jinhua region.

Qiantangjiang basin consists of various rock types from Precambrian metamorphic rocks to Quaternary fluvial sediments, mainly Jurassic sandstone and basic-intermediate volcanic rocks, Silurian-Ordovician sandstone and siltstone, Cambrian carbonates, and Yanshanian intrusive rocks. The Qiantangjiang basin is located in the boundary of the Yangtze Block and the Cathaysia Block, which is separated by the Jiangshan-Shaoxing fault (Xu et al., 2016). The Jiangshan-Shaoxing fault (along the southern Qiangtangjiang main channel) is a boundary line cutting the basin into two stratigraphic regions, which show differences in the composition and development of formations. Due to the orogenic movement in Shengongian Stage and Jinningian Stage, rocks in northwest part of the basin suffered slate-phyllite and greenschist facies metamorphisms, meanwhile, Shengongian Stage and Jinningian Stage intrusive rocks are limited to a few scattered exposures in these areas. Vast areas of Yanshanian granite rocks are exposed in southern basin (Fig. 1). The strata exposed in the catchment are mainly silicate rocks, while only 11.5% of the basin area is covered by carbonate rocks which are mainly distributed in the middle reaches area. According to the Regional Geology of Zhejiang Province and 1:200,000 geological map (ZJBGMR, 1989), there is no evaporites distribution in the Qiantangjiang basin.

3. Sampling and analytical methods

Water samples from mainstream and major tributaries of the Qiantangjiang River were collected in July 2010. The sampling locations are shown in Fig. 1. Water temperature (T), pH and electrical conductivity (EC) were measured in situ using a portable EC/pH meter (YSI-6920, USA). Water samples were collected from the center of the rivers (usually on a bridge) using high density polyethylene (HDPE) containers which were previously acid-washed and cleaned with ultrapure water. Samples were filtered in the field through 0.22 μm pre-cleaned Millipore membrane filter, and the first portion of the filtration was discarded to wash the membrane and filter. Filtered samples were stored in acid-cleaned HDPE bottles and those for the analysis of cations were acidified to pH < 2 with double sub-boiling distilled concentrated HNO_3.

Alkalinity was titrated by hydrochloric acid within 12 h after sample collection. The major cations (Na^+, K^+, Ca^{2+} and Mg^{2+}) were measured using Inductively Coupled Plasma Atomic Emission Spectrometer (ICP-AES) (IRIS Intrepid II XSP, USA). Major anions (Cl^-, F^-, NO_3^- and SO_4^{2-}) were measured by ionic chromatography (IC) (Dionex Corporation, USA). Dissolved silica was determined by spectrophotometry using the molybdate blue method. Reagent and procedural blanks were measured in parallel to the sample treatment, and calibration curve was evaluated by analyses of these quality control standards before, during and after the analyses of a set of samples. Measurement of duplicated sample indicates the analytical error less than ±3%.

4. Results

The pH, temperature, conductivity, major ions, and dissolved SiO_2 in the Qiantangjiang River and its tributaries are given in Table 1. The pH of river waters ranged from 6.85 to 8.96, with an average of 7.59. The water temperature ranged from 22.1 to 31.2 °C. Average conductivity was 153 μS cm^{-1}, ranging from 34 to 308 μS cm^{-1}. With one exception, the total dissolved cations and total dissolved anions were balanced within ±9% of the normalized inorganic charge balance (NICB = $(TZ^+ - TZ^-)/TZ^+$). The total dissolved solid (TDS, mg l^{-1}), expressed here as the sum of major inorganic species concentration ($Na^+ + K^+ + Ca^{2+} + Mg^{2+} + HCO_3^- + Cl^- + SO_4^{2-} + NO_3^- + SiO_2$), is also given in Table 1. The rivers of the Qiantangjiang basin have total dissolved solids (TDS) ranging from 34.6 to 205 mg l^{-1}, with an average of 113 mg l^{-1}, which is comparable with Ganjiang, Songhuajiang and Xishui rivers draining silicate rock dominated region (Chetelat et al., 2008; Liu et al., 2013; Wu et al., 2013), much lower than carbonate dominated river like Wujiang and Xijiang rivers (Han and Liu, 2004; Xu and Liu, 2010). The total cation concentrations (TZ+) are from 317 to 2601 μeq l^{-1}, with an average of 1357 μeq l^{-1}, slightly higher than world river weighted average (TZ+ = 1125 μeq l^{-1}, Meybeck, 2003), and total anion concentrations (TZ−) are from 327 to 2621 μeq l^{-1}, with an average of 1363 μeq l^{-1}.

Major ion compositions are shown in the cation and anion ternary diagrams (Fig. 2). In comparison with rivers (e.g. the Wujiang, Xijiang) which drains in carbonate rock basin, the Qiantangjiang have distinctly higher proportions of Na^+, K^+, and dissolved SiO_2. Among the cations, Ca^{2+} is the dominant cation with concentrations ranging from 81 to 993 μmol l^{-1} and accounts for 35.0–74.1% of the total cations. Na^+ and K^+ vary from 44 to 460 μmol l^{-1} and from 16 to 233 μmol l^{-1}, respectively, and they account for 10.1–59.9% of the total cations. The Mg^{2+} concentration is low in the whole drainage system and is estimated to account approximately 11.5% of the total cations. The anion budget is predominated by HCO_3^-, which ranges from 105 to 1822 μmol l^{-1} and accounts for 23.6–79.1% of the total anion. The second dominant anion is SO_4^{2-} with concentrations ranging from 55 to 437 μmol l^{-1}, and accounts for 5.9–29.5% of the total anion. Cl^- and NO_3^- account for approximately 10.4% and 9.5% of the total anions, respectively. The dissolved SiO_2 concentrations range from 67 to 278 μmol l^{-1} (average of 170 μmol l^{-1}), for the Qiantangjiang main channel, it varied in a narrow range from 137 to 185 μmol l^{-1}.

5. Discussion

5.1. Source of dissolved load

The dissolved species of the river water are the products of weathering of rocks and minerals, atmospheric and anthropogenic inputs in the drainage basin. It is important to constrain the contributions from these sources to the dissolved load in the river waters to derive chemical weathering rates and associated CO_2 consumption within the river basin.

5.1.1. Atmospheric inputs

Chloride, as shown in many studies, is the most common used reference to evaluate atmospheric inputs to rivers (Négrel et al., 1993; Gaillardet et al., 1997; Vries et al., 2001). Two complementary methods can be used for the correction of atmospheric inputs. First, the Cl^- concentration of rainwater at a given point within the basin can be multiplied by the evapotranspiration factor to evaluate the concentration in the river. The second method of determining the atmospheric input of Cl^- in river waters is simply to consider rivers that do not drain any saline formation in pristine area. When there are no salt-bearing rocks in the river basin and anthropogenic inputs can be neglected, the lowest Cl^- concentration in river water could be assumed to be exclusively derived from the atmosphere.

Zhang et al. (2007) and Xu et al. (2011) reported major chemical composition of rainwater at Jinhua and Hangzhou, located within the Qiantangjiang basin (Fig. 1). The Cl^- concentration in rainwater had volume-weighted average value of 8.51 and 13.9 μmol l^{-1}. The

Table 1
Chemical compositions of rivers in the Qiantangjiang basin, East China.

Sample number	Rivers	Date (m-d-y)	T (°C)	EC (μS cm^{-1})	pH	Na^+ (μM)	K^+ (μM)	Ca^{2+} (μM)	Mg^{2+} (μM)	F^- (μM)	Cl^- (μM)	NO_3^- (μM)	SO_4^{2-} (μM)	HCO_3^- (μM)	SiO_2 (μM)	TZ+ (μEq)	TZ− (μEq)	NICB (%)	TDS (mg l^{-1})
	Main stream																		
2	Xinanjiang	7-07-10	31.2	55	7.52	96.2	101	128	41.1	8.89	92.8	57.5	54.9	266	137	537	593	0.33	50.9
3	Xinanjiang	7-07-10	29.1	140	7.82	158	137	404	91.8	12.3	93.7	65.1	147	789	159	1288	1254	2.65	107
24	Xinanjiang	7-10-10	23.8	140	7.24	97.6	69.7	451	81.0	20.0	62.1	109	204	703	164	1231	1302	−5.79	107
23	Fuchunjiang	7-10-10	24.2	123	7.05	130	101	349	66.2	17.7	94.3	124	157	529	169	1061	1079	−1.66	82.1
19	Fuchuanjiang	7-10-10	25.7	141	7.27	163	114	396	69.6	27.3	126	148	161	597	153	1209	1222	−1.13	101
16	Qiantangjiang	7-09-10	27.4	171	7.31	250	233	459	88.7	52.8	206	273	419	335	185	1578	1705	−8.04	132
18	Qiantangjiang	7-10-10	24.9	191	7.76	279	220	524	95.7	22.3	222	244	417	500	165	1738	1821	−4.81	147
	Tributaries																		
1	Xiuninghe	7-07-10	30.9	169	7.89	152	69.4	518	106	14.0	100	74.0	166	930	174	1470	1449	1.42	121
4	Lianjiang	7-07-10	29.1	196	8.43	262	193	564	114	24.7	210	135	121	1373	206	1812	1985	−9.53	163
5	Xiaohe	7-08-10	28.8	190	7.42	347	197	473	106	12.0	303	62.6	147	1130	148	1703	1801	−5.75	144
6	Mianxi	7-08-10	29.4	173	8.92	315	205	453	101	12.0	270	79.7	139	889	134	1626	1529	6.02	126
7	Changyuan	7-08-10	27.9	118	8.27	139	191	317	90.4	12.4	91.4	110	119	596	184	1144	1048	8.35	94.6
8	Dazhouyuan	7-08-10	26.3	95	8.13	136	158	208	79.8	–	74.6	127	81.8	471	179	870	836	3.89	77.3
9	Nameless	7-08-10	27.8	139	8.63	160	70.7	419	81.3	11.9	127	83.9	126	788	74.0	1233	1262	−2.38	100
10	Baiyunxi	7-08-10	27.6	117	8.72	130	143	354	72.5	10.2	105	82.1	104	668	130	1126	1074	4.59	91.9
11	Qiandaolake	7-08-10	25.6	110	8.90	138	86.8	301	69.8	10.2	103	65.4	106	601	66.6	967	992	−2.55	79.0
12	Fuqiangxi	7-09-10	28.4	153	8.96	81.9	220	505	138	12.0	81.2	70.9	123	1071	79.8	1587	1482	6.65	119
13	Fenshuijiang	7-09-10	26.9	174	7.84	156	174	557	126	16.5	137	140	154	974	124	1695	1575	7.05	131
14	Fenshuijiang	7-09-10	26.8	190	7.37	299	218	460	120	12.7	301	202	180	731	167	1677	1605	4.25	132
15	Fenshijiang	7-09-10	23.8	146	7.60	87.5	204	496	80.9	11.7	75.2	124	121	907	156	1446	1360	5.93	119
17	Puyangjiang	7-09-10	27.8	308	7.37	381	233	698	208	41.8	312	223	437	1170	170	2601	2621	−7.97	204
21	Huyuanxi	7-10-10	24.9	114	7.22	165	83.2	264	55.3	13.7	93.1	147	183	263	226	886	884	0.27	78.8
22	Fenshuijiang	7-10-10	26.3	177	7.27	176	135	544	116	15.7	151	142	170	985	175	1632	1634	−0.12	135
25	Lanjiang	7-11-10	23.2	107	7.40	92.5	70.5	327	68.3	14.9	74.9	104	147	486	156	954	975	−2.17	82.2
26	Jinhuajinag	7-11-10	25.8	135	7.02	261	35.4	310	55.6	32.1	185	130	138	468	228	1029	1091	−6.05	91.7
27	Puyangjiang	7-11-10	27.2	221	7.21	460	91.1	504	118	30.3	319	194	268	872	219	1796	1951	−8.61	153
28	Puyangjiang	7-11-10	25.9	129	7.04	193	52.4	338	115	18.3	104	74.0	160	579	189	1152	1095	4.92	93.4
29	Puyangjiang	7-11-10	27.6	281	7.16	361	87.5	469	128	26.8	245	191	239	810	179	1642	1750	−6.62	137
30	Dongyangjiang	7-11-10	25.2	172	6.95	439	71.3	375	66.2	23.3	292	134	202	599	205	1392	1451	−4.24	116
31	Dongyangjiang	7-11-10	27.2	152	7.18	331	15.8	341	70.7	24.3	208	121	182	546	210	1171	1262	−7.76	102
32	Dongyangjiang	7-11-10	26.5	195	6.94	389	77.5	470	81.8	23.5	246	171	232	782	222	1570	1685	−7.33	136
33	Wuyijiang	7-11-10	26.5	140	7.02	275	120	319	60.7	36.2	199	150	180	437	236	1155	1182	−2.30	100
34	Qujiang	7-12-10	24.2	99	7.05	205	114	285	58.3	14.6	191	114	132	305	278	1005	888	11.6	85.4
36	Wuxijiang	7-12-10	22.1	34	6.85	56.8	78.9	80.9	9.8	13.1	32.8	60.6	57.6	105	161	317	327	−2.95	34.6
37	Jiangshangang	7-12-10	27.0	102	7.05	123	133	284	49.8	18.6	86.5	123	144	377	183	924	893	3.39	79.4
38	Changshangang	7-12-10	23.9	131	7.17	65.2	89.1	409	111	–	56.8	95.0	170	687	165	1195	1179	1.38	100
39	Zitongyuan	7-12-10	24.2	260	7.99	50.0	85.4	993	212	–	66.8	153	235	1822	172	2546	2512	1.35	205
40	Yuchuan	7-12-10	24.6	231	7.86	43.5	88.4	859	189	–	55.1	97.6	169	1763	170	2228	2253	−1.11	185
41	Jinpuxi	7-12-10	22.7	131	7.69	44.1	81.0	458	113	–	19.1	95.2	107	920	143	1266	1248	1.43	107
42	Wuqianxi	7-12-10	24.5	106	7.65	61.1	98.3	335	87.9	–	37.2	68.3	112	663	164	1005	992	1.35	87.3
43	Majinxi	7-12-10	23.7	125	7.46	64.3	108	406	117	–	25.9	75.0	174	687	164	1218	1136	6.71	98.9
44	Majinxi	7-13-10	24.1	139	7.33	59.8	116	429	136	–	29.6	80.4	209	752	162	1305	1281	1.87	108

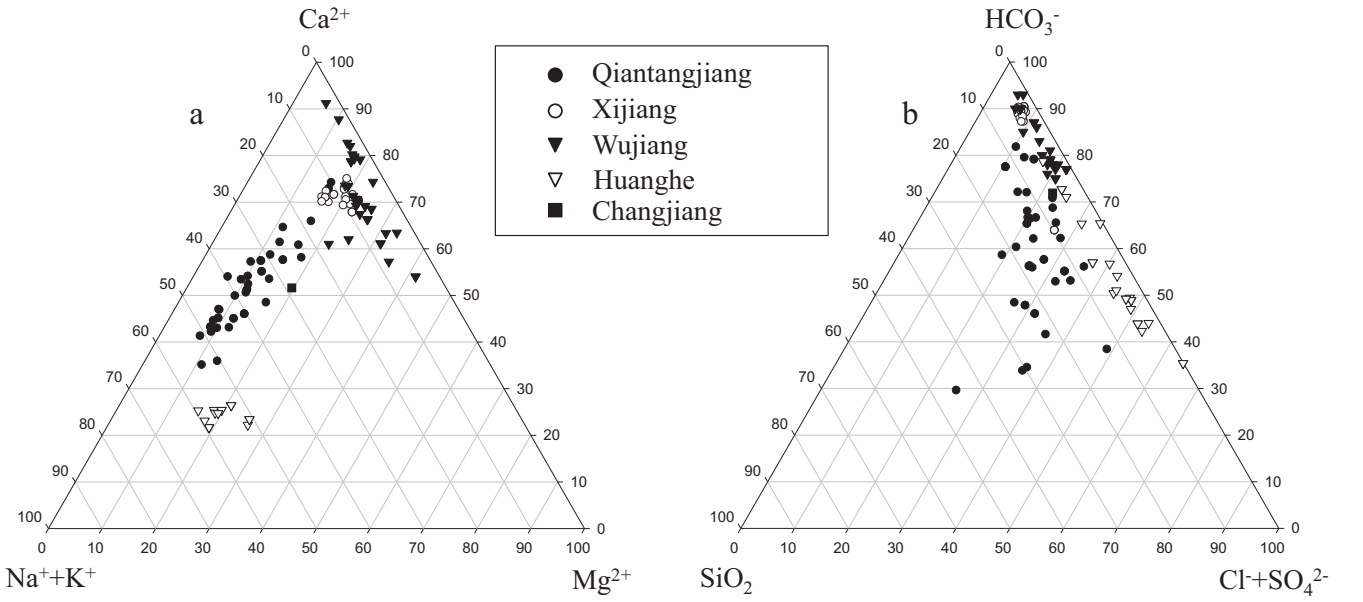

Fig. 2. Ternary diagrams showing cation (diagram a) and anion and Si (diagram b) compositions of the Qiantangjiang River waters. Also shown are chemical compositions of major ions of some other large rivers in China for a comparison. Data source for Xijiang, Xu and Liu (2007, 2010), Wujiang, Han et al. (2010), Changjiang, Chetelat et al. (2008), and Huanghe, Fan et al. (2014).

mean annual precipitation and mean annual evaporation of Qiantang River basin is about 1600 mm and 800 mm, so we take 2 as the evapotranspiration factor. So the atmospheric contribution of Cl^- to river water can be estimated to be 17–28 μmol l^{-1}. In the Qiantangjiang River system, river waters with the lowest Cl^- concentration were mainly found around the Qiandao Lake. According to the geologic setting (Fig. 1) (ZJBGMR, 1989), there is no salt-bearing rock in this area. In addition, the area is sparsely populated and over 90% of the area is forested. Therefore, we assumed that the lowest Cl^- concentration (19 μmol l^{-1}) in river water, originates only from the atmosphere.

The data of rainwater from Jinhua and Hangzhou within the Qiantangjiang basin were compiled and the Cl-normalized molar ratios are listed in Table 2. According to these studies, the contribution of sea-salt was minor in the rain water and the high concentrations of SO_4^{2-} and NO_3^- reflected the importance of anthropogenic emissions to the atmosphere (Zhang et al., 2007; Xu et al., 2011). In these precipitation studies, the SO_4^{2-}/Na^+ and NO_3^-/Na^+ molar ratios ranged from 4.5 to 7.6 and from 3.1 to 5.0, indicating S and N enrichment of rainwater with respect to sea-salt ($SO_4^{2-}/Na^+ = 0.06$, $NO_3^-/Na^+ = 0$). In addition, the concentrations of SO_4^{2-} and NO_3^- ions in precipitation were higher at Hangzhou and Shanghai than at Jinhua, implying a more intensive contribution of human activities to precipitation of big city. By using the average Cl-normalized ratios of rainwater in Table 2, proportions of other elements can be corrected for the contribution of atmospheric deposition. On this basis, 9.8% (4.8–32%) of total dissolved cations originate from rain in the Qiantangjiang River. Among the anions, SO_4^{2-} and NO_3^- appear to be derived mainly from the atmosphere; about 59.7% (20.8–100%) of SO_4^{2-} and 58.5% (22.3–100%) of NO_3^- were contributed by atmospheric input in the Qiantangjiang River.

5.1.2. Anthropogenic inputs

Zhejiang province is one of the most economically developed areas in China and has a high population density in the lower reach of the studied basin, the water chemistry could be significantly impacted by human activities. Human activities can generate various contamination sources, including atmospheric transport and fertilizer application, and urban and industrial wastewaters (Grosbois et al., 2000). As discussed above, the atmospheric loading in the Qiantangjiang basin may have significant anthropogenic inputs, especially for SO_4^{2-} and NO_3^-. It is well known that NO_3^- and Cl^- are commonly derived from agricultural fertilizers, animal waste, and municipal and industrial sewage (Grosbois et al., 2000; Han and Liu, 2004; Chetelat et al., 2008). The water samples present high NO_3^- concentrations with NO_3^-/Na^+ molar ratios of 0.87, much higher than those in most of the world large rivers (Gaillardet et al., 1999), and close to the value of 0.6 for the waste water sample collected in lower reaches of the Changjiang reported by Chetelat et al. (2008). Significant variations of NO_3^- and Cl^- concentrations can be observed from upstream to downstream, and there is a sharp increase of both NO_3^- and Cl^- concentration downstream of Hangzhou area, the biggest city in the Qiantangjiang basin (Table 1). Meanwhile, the tributaries draining from the Jinhua-Quzhou basin also have high concentrations of NO_3^- and Cl^- (sample 26–34). The Jinhua-Quzhou basin is the most developed industry and agriculture region with a high density of population in Zhejiang. Given the absence of evaporites in the Qiantangjiang basin, the excess Cl^- corrected for atmospheric inputs could be ascribed to the human activities.

The river waters studied here are also rich in SO_4^{2-}, showing significantly high SO_4^{2-}/Na^+ ratios (average of 1.28). The SO_4^{2-} in the river waters may have several sources, such as human activities,

Table 2
Cl-normalized molar ratios in precipitation from two sites within the Qiantangjiang basin.

Site	K/Cl	Na/Cl	Ca/Cl	Mg/Cl	SO_4^{2-}/C1	NO_3^-/Cl	References
Jinhua	0.56	0.74	2.81	0.20	5.59	3.67	Zhang et al. (2007)
Hangzhou	0.30	0.88	1.87	0.25	3.96	2.76	Xu et al. (2011)
Average	0.43 ± 0.13	0.81 ± 0.07	2.34 ± 0.47	0.23 ± 0.03	4.78 ± 0.82	3.21 ± 0.45	

dissolution of gypsum, oxidation of sulfides, and acid deposition. In estimating CO_2 consumption rates, distinguishing these sources is very important as the latter two can generate protons and take over carbonic acid in carbonate and silicate weathering reactions (Han and Liu, 2004; Moon et al., 2007; Xu and Liu, 2007, 2010; Li et al., 2008; Chetelat et al., 2008). Good linear correlation is observed between the molar ratios of SO_4^{2-}/Na^+ and NO_3^-/Na^+ ($R^2 = 0.81$) in river waters (Fig. 3). This suggests that SO_4^{2-} and NO_3^- have a common source which could be anthropogenic inputs since NO_3^- is most likely of anthropogenic origin. The molar ratios of SO_4^{2-}/Na^+ and NO_3^-/Na^+ in rainwater from Jinhua and Hangzhou, located within the Qiantangjiang basin, are also shown in Fig. 3 (data from Zhang et al., 2007; Xu et al., 2011), and they have higher ratios than river waters. Because of the co-emission of their precursors SO_2 and NO_x, the obvious positive correlation between SO_4^{2-}/Na^+ and NO_3^-/Na^+ would reflect the input of these pollutants from fossil fuel combustion. Huang et al. (2008) also reported rainwater collected at Zhejiang, Shanghai, and Nanjing with high concentration of SO_4^{2-} (58–120 μmol l^{-1}) with pH normally lower than 4.5. Therefore, the high content of SO_4^{2-} in the rain waters of Eastern China implies that acid rain has a significant influence on water chemistry in the studied area. Huge emissions of SO_2 and NO_x are accompanied with the rapid economic development in China, and especially Zhejiang is one of the most heavily acid rain polluted regions in China for many years (Wang et al., 2000; Larssen and Carmichael, 2000; Han et al., 2006; Larssen et al., 2006; Huang et al., 2008).

Other possible anthropogenic source of SO_4^{2-} could be the wastewaters from industry, agriculture and urban resident, considering the fact that the high density of population and developed industry and agriculture in Zhejiang province. The SO_4^{2-}/Na^+ ratio is 0.17 ± 0.10 for the wastewater samples collected from paddy fields and municipal sewage (our unpublished data). It is estimated that 11.5% (0–32.9%) of SO_4^{2-} originate from human activities in the Qiantangjiang River. We assume that the remaining SO_4^{2-} could derive from the oxidation of sulfide minerals as volcanogenic and coal-bearing sedimentary rocks are widely distributed in the catchment, while no evaporites in the Qiantangjiang basin has been reported.

5.1.3. Chemical weathering inputs

The samples were displayed on a plot of Na-normalized molar ratios (Fig. 4), the best correlations were observed between

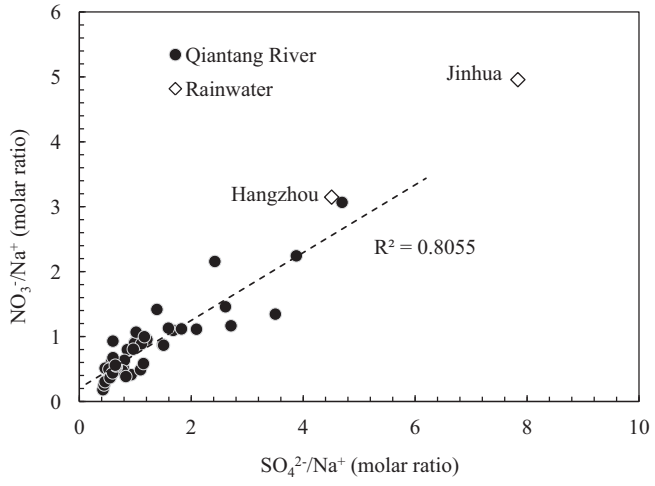

Fig. 3. Plots showing variations of SO_4^{2-}/Na^+ with NO_3^-/Na^+ molar ratios of the Qiantangjiang River waters. The volume-weighted mean molar ratio of Jinhua and Hangzhou rainwater (Zhang et al., 2007; Xu et al., 2011) are also shown.

Ca^{2+}/Na^+ and Mg^{2+}/Na^+ ($R^2 = 0.97$, n = 42) and Ca^{2+}/Na^+ and HCO_3^-/Na^+ ($R^2 = 0.99$, n = 42). The distribution of present samples in the figure shows a mixing trend between carbonate and silicate weathering. This corresponds with the distribution of rocks in the basin. In addition, all water samples have equivalent ratios of $[Na^+ + K^+]/Cl^-$ larger than one, indicating Na^+ and K^+ mainly derived from silicate weathering rather than evaporites dissolution. The characteristics of the silicate and carbonate end-members can be deduced from the correlations between elemental ratios and referred to literature data based on simple and well-constrained lithology. After correction for atmospheric inputs, the Ca^{2+}/Na^+, Mg^{2+}/Na^+ and HCO_3^-/Na^+ of the river samples ranged from 0.77 to 30, 0.13 to 6.6, and 1.4 to 65.7, respectively. Although the value in the Dongyang River (sample 30, 0.78 for Ca^{2+}/Na^+ and 0.15 for Mg^{2+}/Na^+) can be considered to reflect the draining of silicates, using the high $(Ca^{2+} + Mg^{2+})/Na^+_{sil}$ ratios (0.93) may overestimate the silicate contribution. Several previous researches have reported the chemical composition of rivers, such as the Amur and the Songhuajiang in North China, the Xishui in the lower reaches of the Changjiang, and the Han and six major rivers in South Korea (Moon et al., 2009; Liu et al., 2013; Wu et al., 2013; Ryu et al., 2008; Shin et al., 2011). Since the similar geological setting between these river basins and the study area, we could better constrain the composition of silicate end-member according to their results. The Ca^{2+}/Na^+ and Mg^{2+}/Na^+ ratio of silicate endmember has been reported for the Amur (0.36 and 0.22), the Songhuajiang (0.44 and 0.16), the Xishui (0.65 and 0.32), the Han (0.55 and 0.21) and major rivers in South Korea (0.48 and 0.20) in the studies above. Thus, in the present study, we used Ca^{2+}/Na^+ of 0.54 ± 0.14 and Mg^{2+}/Na^+ of 0.20 ± 0.06 (by averaging the data documented by the above publication) as the silicate end-member. In many watersheds of the world, it has been demonstrated that weathering of carbonate minerals is more important than the weathering of silicate minerals in controlling river water chemistry (e.g. Roy et al., 1999; Ryu et al., 2008). As revealed by the high concentrations of both dissolved Ca^{2+} and HCO_3^-, the ionic composition is controlled by the weathering of carbonates in the Qiantangjiang basin. The samples collected in the upper reaches (No. 39 and 40) fall close to the carbonate endmember, and we adopted the Ca^{2+}/Na^+ of 50 ± 20 and Mg^{2+}/Na^+ of 10 ± 4.0 as the carbonate end-member (Gaillardet et al., 1999).

5.1.4. Contribution of different sources

To quantify the contribution of atmosphere, anthropogenic inputs, and rock weathering in the Qiantangjiang River waters, a straight forward method is employed in this study (Galy and France-Lanord, 1999; Moon et al., 2007; Xu and Liu, 2010). The solutes in rivers are a mixture of atmospheric inputs, anthropogenic inputs and weathering of silicate, carbonate and evaporites. So, the mass budget equation for any element X in the river water (in molar concentration) can be written as:

$$[X]_{riv} = [X]_{atm} + [X]_{anth} + [X]_{eva} + [X]_{sil} + [X]_{carb} \quad (1)$$

The calculations are based on some straightforward simplifications of the budget equations. Given the absence of evaporites in the study area, only rain, anthropogenic inputs, carbonate and silicate weathering were considered. First, it is assumed that Cl^- in the river water is of atmospheric and anthropogenic origin and the Cl^- in the lowest Cl^- content (19 μmol l^{-1}) river water sample originate only from rainwater. We calculated the input of the cations from rain by using the Cl-normalized ratios of local rain in Table 2. Second, the excess of Cl^- over atmospheric input is considered to be anthropogenic and balanced by Na^+. Third, all Na^+ after the atmospheric and anthropogenic corrections and all K^+ after the atmospheric correction were assumed to be from silicate weathering. The Ca^{2+}/Na^+ ratio of 0.54 ± 0.14 and Mg^{2+}/Na^+ ratio of 0.20 ± 0.06 for silicate end-member are used to calculate the

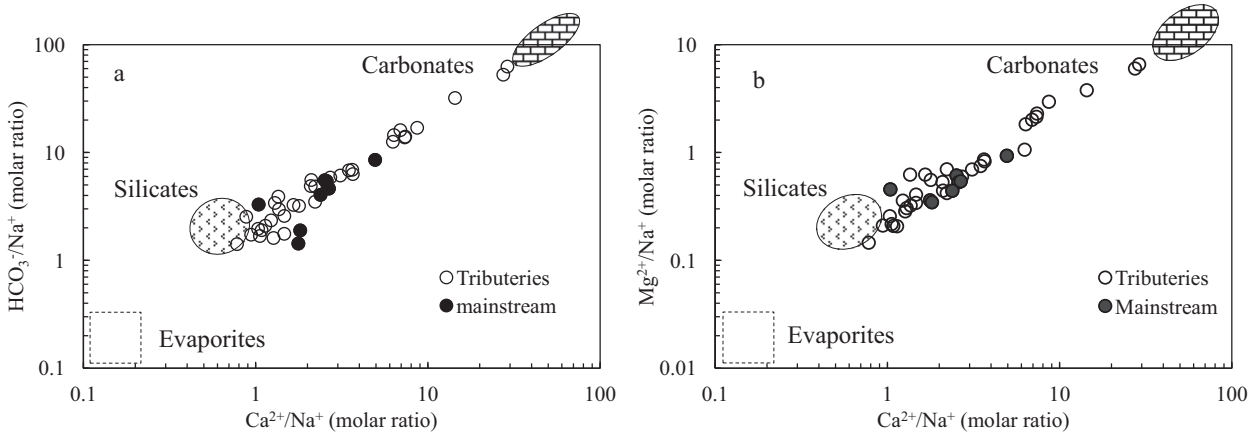

Fig. 4. Plots of HCO_3^-/Na^+ vs. Ca^{2+}/Na^+ (a) and Mg^{2+}/Na^+ vs. Ca^{2+}/Na^+ (b) for the Qiantangjiang River waters, showing mixing between silicate and carbonate end-members. The compositions for silicate and carbonate end-member are discussed in the text.

contribution of silicate weathering as discussed above. The final estimation of carbonate weathering input was made by subtracting the rain and silicate contributions from the total dissolved Ca^{2+} and Mg^{2+}.

The calculated contributions of different sources to the total cationic load for the Qiantangjiang main channel and its main tributaries are illustrated in Fig. 5. The calculated results shows that rain accounts for 9.8% (4.8–32%), anthropogenic 13.9% (0–28.7%), silicate 25.6% (5.8–53%), and carbonate 50.7% (9.4–86%) of the total dissolved cations on a molar basis. The propagated uncertainties for cationic fractions of the different reservoirs were also calculated, the results are ±1.8% (from ±0.9 to ±5.9%), ±1.9% (from ±0.2 to ±4.5%), and ±2.7% (from ±0.7 to ±6.5%) for rain, silicate, and carbonate, respectively. Generally, the dissolved cation load of the rivers in the study area is dominated by both carbonate and silicate weathering, which together account for about 76.3% of the total cationic load. It is notable that the contribution of carbonate weathering to the dissolved cation load averages 50.7% even though no obvious distribution of carbonates is found in the river basin. The highest contribution to the dissolved cation load from silicate weathering are observed in the Wuxijiang River (52.5%, sample 36), draining an area mainly covered by granitic and volcanic rocks. There is a general increase of anthropogenic contribution from upstream to downstream, and high anthropogenic contribution (>20%) is observed in samples 26, 27, 29–34 from the Puyangjiang, Dongyangjiang, Wuyijiang, Jinhuajiang, and Qujiang rivers in the south of the Qiantangjiang River (Fig. 5), flowing through the most developed area of the basin with a higher population density. This trend illustrates the great sensitivity of the Qiantangjiang to the changes of land use in spite of the high water discharge of this river.

5.2. Chemical weathering and CO_2 consumption rates

The chemical weathering rate of silicate and carbonate is estimated by the mass budget and surface area and average annual

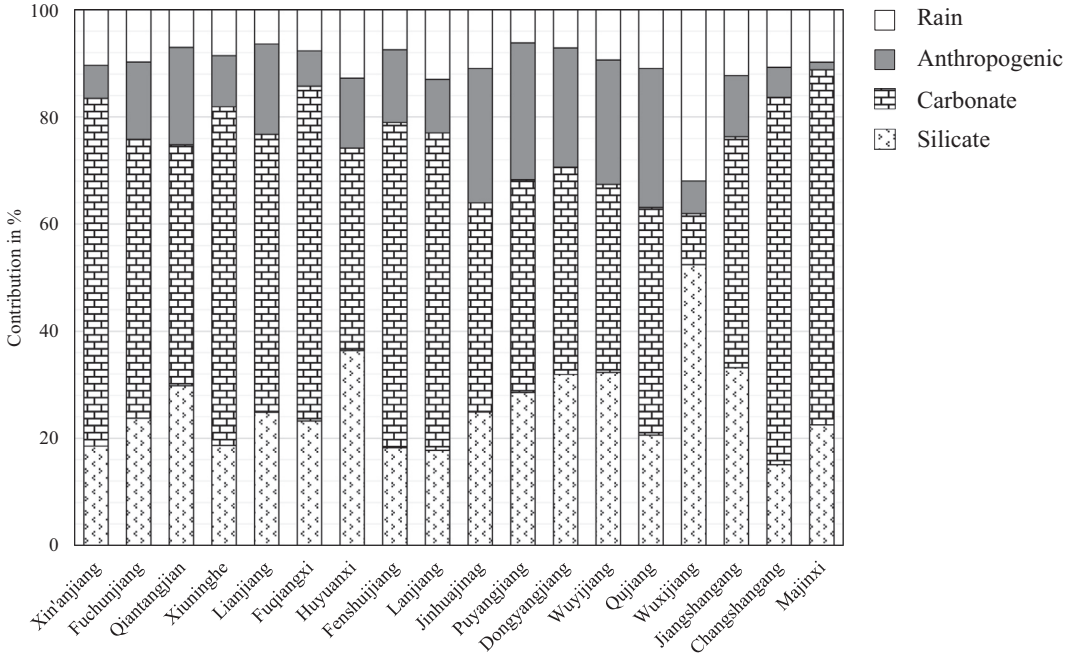

Fig. 5. Calculated contributions (in%) from the different reservoirs to the total cationic load for the Qiantangjiang main stream and its major tributaries. The cationic load is equal to the sum of K^+, Na^+, Ca^{2+} and Mg^{2+} from the different reservoirs.

discharge available from the basin, expressed in ton km^{-2} a^{-1}. The chemical weathering rate of silicates (SWR) is calculated using the Na^+, K^+, Ca^{2+} and Mg^{2+} concentrations from silicate weathering and assuming that all dissolved SiO_2 is derived from silicate weathering (Xu and Liu, 2010). The assumption could overestimate the silicate weathering rate, because a part of silica may come from biological activity (Millot et al., 2003).

$$SWR = ([Na]_{sil} + [K]_{sil} + [Ca]_{sil} + [Mg]_{sil} + [SiO_2]_{riv}) \times discharge/area \quad (2)$$

The rate of carbonate weathering (CWR) is calculated based on the sum of Ca^{2+} and Mg^{2+} and HCO_3^- from carbonate weathering, with half of the HCO_3^- from carbonate weathering being derived from the atmosphere CO_2.

$$CWR = ([Ca]_{carb} + [Mg]_{carb} + 1/2[HCO_3]_{carb}) \times discharge/area \quad (3)$$

Samples 24, 23, and 19 collected from the main channel were used to calculate the rock weathering and CO_2 consumption rates of the upper reaches (Xin'anjiang), the middle reaches (Fuchunjiang), and the whole Qiantangjiang basin, respectively. We also calculated cationic weathering rates for silicate and carbonate rocks ($Cation_{sil}$ and $Cation_{carb}$), and results are listed in Table 3. The carbonate weathering rate (CWR) is variable from one sub-basin to another and ranges from 1.77 ton km^{-2} a^{-1} for Wuxijiang to 36.2 ton km^{-2} a^{-1} for Fenshuijiang. The total rock weathering rate (TWR) for the Qiantangjiang basin is 41.1 ton km^{-2} a^{-1}, 1.7 times as the world average (24 ton km^{-2} a^{-1}) estimated by Gaillardet et al. (1999). The cation-silicate weathering rate ($Cation_{sil}$) ranges from 3.11 ton km^{-2} a^{-1} for Lanjiang to 7.47 ton km^{-2} a^{-1} for Puyangjiang. For the Qiantangjiang main channel, the cation-silicate weathering rate increases slightly from upstream to downstream, from 2.66 ton km^{-2} a^{-1} at Meicheng to 4.90 ton km^{-2} a^{-1} at Hangzhou. This increase may be attributed to the increasing runoff and temperature from upstream to downstream in the river basin. Further, a good linear correlation ($R^2 = 0.75$) between the SWR and runoff is observed for river basins draining silicate area in eastern Asia (Fig. 6). For silicate weathering, many studies have reported a similar correlation between runoff and weathering rates (e.g., Gaillardet et al., 1999; White et al., 1999; Millot et al., 2002; Oliva et al., 2003; Wu et al., 2013; Pepin et al., 2013), and the chemical weathering rates of Qiantangjiang basin comply with the pattern.

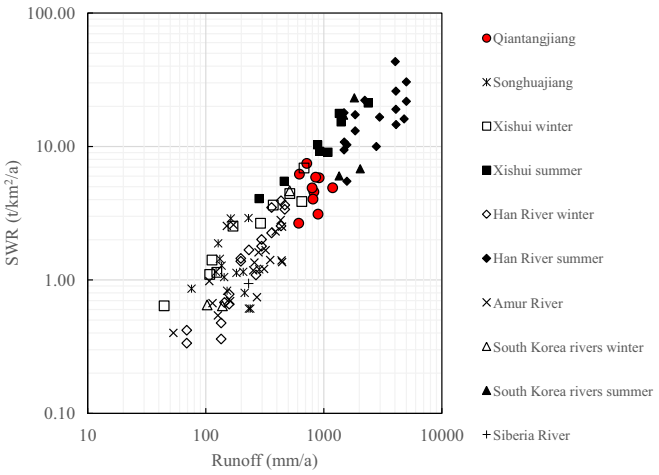

Fig. 6. Plots of the cationic-silicate weathering rate ($Cation_{sil}$) vs. runoff showing that chemical weathering rates are positively correlated with runoff. For comparison, SWR are given for other rivers in East Asia, e.g. the Songhuajiang River (Liu et al., 2013), the Xishui River (Wu et al., 2013), the Amur River (Moon et al., 2009) in China, the Han River (Ryu et al., 2008), major rivers in South Korea (Shin et al., 2011), and the Siberia River (Huh and Edmond, 1999).

To calculate atmospheric CO_2 consumption by silicate weathering (CSW), we assumed that both silicate-derived alkalinity and silicate derived cations were in a charge-balanced state (Roy et al., 1999).

$$[CO_2]_{SW} = [HCO_3]_{SW} = [Na]_{sil} + [K]_{sil} + 2[Ca]_{sil} + 2[Mg]_{sil} \quad (4)$$

The consumption of CO_2 by carbonate weathering (CCW) is calculated as follows:

$$[CO_2]_{CW} = [HCO_3]_{CW} = [Ca]_{carb} + [Mg]_{carb} \quad (5)$$

In addition to CO_2, protons from other acids (e.g. sulfuric acid) dissociation can increase the weathering rates and need to be considered for the weathering fluxes calculation (Lerman and Wu, 2006; Lerman et al., 2007). Several studies have shown that H_2SO_4 plays an important role in rock weathering (Galy and France-Lanord, 1999; Karim and Veizer, 2000; Yoshimura et al., 2001; Han and Liu, 2004; Spence and Telmer, 2005; Lerman and Wu, 2006; Li et al., 2008, 2014; Xu and Liu, 2007, 2010). Sulfuric acid can be generated by natural oxidation of pyrite and

Table 3
Chemical weathering and associated CO_2 consumption rates for the Qiantangjiang main channel and main tributaries.

River	Discharge	Area	Source of cations				Silicates		Carbonates		Total rock weathering	CO_2 consumption rate			
			Rain	Pollu.	Sil.	Carb.	$Cation_{sil}$[a]	SWR[b]	$Cation_{carb}$[a]	CWR[b]	TWR[b]	CSW[c]	CCW[c]	SSW[d]	SCW[d]
	(10^9 m^3 a^{-1})	(10^3 km^2)	(%)				(ton km^{-2} a^{-1})					(10^3 mol km^{-2} a^{-1})			
Main channel															
Xin'anjiang	7.23	11.8	10.4	6.2	18.6	64.9	2.66	8.71	10.5	18.8	27.5	98	278	61.5	175
Fuchunjiang	31.54	38.3	11.2	11.7	24.9	52.2	4.57	13.4	12.0	21.6	35.0	170	318	120	225
Qiantangjiang	44.25	55.6	9.7	14.4	23.8	52.0	4.90	16.2	13.9	24.9	41.1	273	369	211	286
Main tributaries															
Fenshuijiang	3.13	3.43	7.4	13.6	18.2	60.7	5.83	15.4	20.0	36.2	51.6	181	538	143	423
Lanjiang	17.28	19.35	13.0	10.0	17.8	59.2	3.11	11.5	11.0	19.9	31.4	103	295	66.5	191
Jinhuajiang	5.3	6.551	10.9	25.1	25.0	39.0	4.04	15.1	7.9	14.2	29.3	181	209	128	147
Puyangjiang	2.46	3.431	6.2	25.6	28.6	39.7	7.47	16.9	12.4	22.5	39.4	318	334	218	229
Dongyangjiang	0.874	1.407	7.1	22.3	32.0	38.7	6.21	14.5	9.3	16.7	31.2	270	245	185	167
Wuxijiang	3.076	2.59	32.0	6.1	52.5	9.4	4.91	16.4	1.02	1.77	18.1	166	25.3	65.3	9.95
Jiangshangang	1.68	1.97	12.3	11.4	33.2	43.1	5.89	15.3	8.19	14.70	30.0	193	217	124	139

[a] $Cation_{sil}$ and $Cation_{carb}$: the sum of cation concentrations derived from silicate weathering and carbonate weathering.
[b] SWR, CWR and TWR represent silicate weathering rate, carbonate weathering rate and total weathering rates, respectively.
[c] CO_2 consumption associated with the weathering only by carbonic acid (see Section 5.2).
[d] Estimated CO_2 consumption including the weathering by sulfuric acid (see Section 5.2).

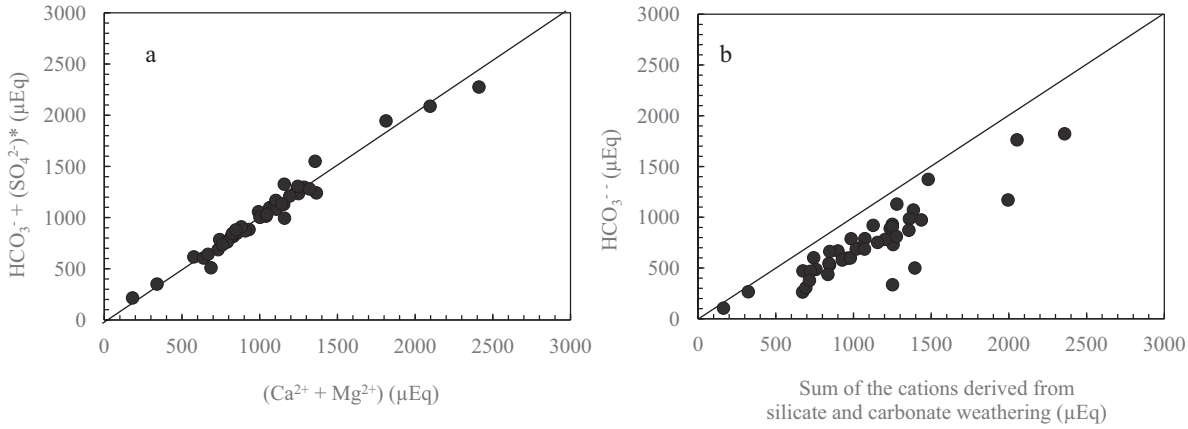

Fig. 7. Plots of $HCO_3^- + (SO_4^{2-})^*$ vs. $Ca^{2+} + Mg^{2+}$ (a) and HCO_3^- vs. the sum of the cations derived from carbonate and silicate weathering (b) for the Qiantangjiang River waters. $(SO_4^{2-})^*$ is the sulfate concentration subtracted by the contribution of human activities from river water.

anthropogenic emissions of SO_2 from coal combustion and the H_2SO_4 product can then dissolve carbonate and silicate minerals. Reactions of H_2SO_4 with carbonate and silicate minerals are described according to Lerman et al. (2007), Calmels et al. (2007) and Chetelat et al. (2008) as follows:

$$H_2SO_4 + 2CaCO_3 = 2Ca^{2+} + SO_4^{2-} + 2HCO_3^-$$

$$H_2SO_4 + H_2O + CaSiO_3 = Ca^{2+} + SO_4^{2-} + H_4SiO_4$$

According to these reactions, no atmospheric CO_2 is consumed when carbonate and silicate are weathered by sulfuric acid. From a long-term perspective, coupled sulfuric carbonate weathering (SCW) followed by carbonate deposition in the oceans acts as a net release of CO_2 into the atmosphere (Spence and Telmer, 2005; Calmels et al., 2007; Li et al., 2008). And, the drawdown of CO_2 by silicate weathering would be overestimated when sulfuric silicate weathering (SSW) is ignored (Spence and Telmer, 2005; Xu and Liu, 2007, 2010; Shin et al., 2011), especially in areas highly impacted by acid deposition. Therefore, deciphering the sources of protons is crucial to estimate the CO_2 consumption by rock weathering. As documented above, Zhejiang is one of the most heavily acid rain-impacted areas in China for many years. It is easily verified by the stoichiometry between cations and anions. Evidence of the involvement of protons originating from H_2SO_4 in the Qiantangjiang River is given in Fig. 7. In the river waters, total $Ca^{2+} + Mg^{2+}$ could not be balanced by HCO_3^- alone; instead, it required significant additional SO_4^{2-} to achieve ionic balance. In the absence of evaporite minerals, and also deducting sulfate from human activities (communal/industrial inputs and agriculture) (the deducted results are expressed as $(SO_4^{2-})^*$), almost all data points are on the 1:1 line (Fig. 7a), suggesting that sulfuric acid plays an important role in rock weathering of the river basin. A different way of presenting this result is to plot the HCO_3^- concentrations as a function of the cations released by silicate and carbonate weathering (Fig. 7b), the theoretical line is 1:1 for chemical weathering reactions in the case where only CO_2 is involved. Data in this study deviate far from the theoretical line 1:1, indicating the contribution of H_2SO_4 to weathering reactions. Thus, the rate of CO_2 consumption during silicate and carbonate weathering can be determined from the equation of Moon et al. (2007) and Ryu et al. (2008), as follows:

$$[CO_2]_{SSW} = [Cation]_{sil} - \gamma \times 2[SO_4] = [Na]_{sil} + [K]_{sil} + 2[Ca]_{sil} + 2[Mg]_{sil} - \gamma \times 2[SO_4] \quad (6)$$

$$[CO_2]_{SCW} = [Cation]_{Carb} - (1-\gamma) \times [SO_4] = [Ca]_{carb} + [Mg]_{carb} - (1-\gamma) \times [SO_4] \quad (7)$$

where γ is an adjustment factor, and calculated by $cation_{sil}/(cation_{sil} + cation_{carb})$.

The calculated CO_2 consumption rates by rock weathering of the Qiantangjiang main channel and its main tributaries are shown in Table 3. CO_2 consumption rates by carbonate weathering and silicate weathering by carbonic acid (CCW and CSW, respectively) are between 25.3×10^3 and 538×10^3 mol km^{-2} a^{-1} and between 103×10^3 and 318×10^3 mol km^{-2} a^{-1} for the main tributaries. For the whole river basin CCW and CSW are 369×10^3 mol km^{-2} a^{-1} and 273×10^3 mol km^{-2} a^{-1}, respectively. Assuming that sulfate from the waste-water does not participate in the weathering of rocks, we estimate the concentration of H_2SO_4 involved in chemical weathering reactions of carbonate and silicate in rivers of the Qiantangjiang catchment. With the assumption that the proportion of H_2SO_4 involved in carbonate weathering and silicate weathering reactions is equal to $cation_{sil}/(cation_{sil} + cation_{carb})$, CO_2 consumption rates by H_2SO_4-induced carbonate weathering (SCW) and silicate weathering (SSW) are between 9.95×10^3 and 423×10^3 mol km^{-2} a^{-1} and between 65.3×10^3 and 218×10^3 mol km^{-2} a^{-1} for the main tributaries. For the whole Qiantangjiang basin, CO_2 consumption rates by H_2SO_4-induced carbonate and silicate weathering is 286×10^3 mol km^{-2} a^{-1} and 211×10^3 mol km^{-2} a^{-1}, respectively. These results highlight the fact that the drawdown of CO_2 by carbonate and silicate weathering can be overestimated when the involvement of sulfuric acid is ignored. The CO_2 consumption rates for carbonate and silicate weathering are 77% of the value when we assume that all the protons in the weathering reactions are provided by carbonic acid after deducting the contribution from sulfuric acid weathering.

6. Conclusions

The major ionic compositions of the Qiantangjiang River were investigated, and the river waters have high SO_4^{2-} content, showing significantly higher SO_4^{2-}/Na^+ ratios than most of the world large rivers. Two main sources of SO_4^{2-} in river waters were identified as acid precipitation and the oxidation of sulfide minerals, with more than 59.7% of the SO_4^{2-} derived from acid rain. Source identification of the river waters suggested that four major reservoirs (carbonates, silicates, atmospheric and anthropogenic inputs) contribute to the dissolved solutes. The dissolved cation loads

originated mostly from carbonate and silicate weathering, which together account for about 76.3% of the total cationic load of the river water.

The cationic chemical weathering rates of silicate and carbonate for the Qiantangjiang basin are estimated to be approximately 4.9 ton km^{-2} a^{-1} and 13.9 ton km^{-2} a^{-1}, respectively. Compared to rivers draining silicate rocks in eastern Asia, the Qiantangjiang basin is characterized by moderate silicate weathering rates, and a positive correlation exists between the cationic silicate weathering rates and runoff. H_2SO_4 from acid precipitation is involved as a proton donor in weathering reactions in the Qiantangjiang basin. The estimated CO_2 consumption rates for the Qiantangjiang basin decrease by 83×10^3 mol km^{-2} a^{-1} and 61×10^3 mol km^{-2} a^{-1}, respectively, when H_2SO_4 involvement in carbonate and silicate weathering reactions is considered. That is a 23% decrease of the value before deducting the H_2SO_4. This result for the first time quantitatively highlights the fact that, in one of the most serious acid deposition affected basin in China, the drawdown of CO_2 by carbonate and silicate weathering will be largely overestimated if the role of sulfuric acid is not evaluated.

Acknowledgements

This work was financially supported by the National Basic Research Program of China (“973 Program”, Grant No. 2013CB956401), the “Strategic Priority Research Program” of the Chinese Academy of Sciences (Grants No. XDB03020400 and XDB15010405), Natural Science Foundation of China (No. 41173114 and 41402323). Wenjing Liu acknowledges international postdoctoral exchange fellowship program (No. 20140045) and support from China postdoctoral council. The authors appreciate the insightful comments and constructive suggestions from the handling editor and the anonymous reviewers.

References

Amiotte-Suchet, P., Probst, A., Probst, J.-L., 1995. Influence of acid rain on CO_2 consumption by rock weathering: local and global scales. Water Air Soil Pollut. 85, 1563–1568.

Amiotte-Suchet, P., Probst, J.-L., Ludwig, W., 2003. Worldwide distribution of continental rock lithology: implications for the atmospheric/soil CO_2 uptake by continental weathering and alkalinity river transport to the oceans. Global Biogeochem. Cycles 17, 1038–1052.

Berner, R.A., Caldeira, K., 1997. The need for mass balance and feedback in the geochemical carbon cycle. Geology 25, 955–956.

Calmels, D., Gaillardet, J., Brenot, A., France-Lanord, C., 2007. Sustained sulfide oxidation by physical erosion processes in the Mackenzie River basin: climatic perspectives. Geology 35, 1003–1006.

Calmels, D., Galy, A., Hovius, N., Bickle, M., West, A.J., Chen, M.-C., Chapman, H., 2011. Contribution of deep groundwater to the weathering budget in a rapidly eroding mountain belt, Taiwan. Earth Planet. Sci. Lett. 303, 48–58.

Chetelat, B., Liu, C., Zhao, Z., Wang, Q., Li, S., Li, J., Wang, B., 2008. Geochemistry of the dissolved load of the Changjiang Basin rivers: anthropogenic impacts and chemical weathering. Geochim. Cosmochim. Acta 72, 4254–4277.

Fan, B.L., Zhao, Z.Q., Tao, F.X., Liu, B.J., Tao, Z.H., Gao, S., He, M.Y., 2014. Characteristics of carbonate, evaporite and silicate weathering in Huanghe River basin: a comparison among the upstream, midstream and downstream. J. Asian Earth Sci. 96, 17–26.

Gaillardet, J., Dupré, B., Allègre, C.J., Négrel, P., 1997. Chemical and physical denudation in the Amazon River basin. Chem. Geol. 142, 141–173.

Gaillardet, J., Dupré, B., Louvat, P., Allegre, C.J., 1999. Global silicate weathering and CO_2 consumption rates deduced from the chemistry of large rivers. Chem. Geol. 159, 3–30.

Galy, A., France-Lanord, C., 1999. Weathering processes in the Ganges-Brahmaputra basin and the riverine alkalinity budget. Chem. Geol. 159, 31–60.

Gandois, L., Perrin, A.-S., Probst, A., 2011. Impact of nitrogenous fertiliser-induced proton release on cultivated soils with contrasting carbonate contents: a column experiment. Geochim. Cosmochim. Acta 75, 1185–1198.

Gislason, S.R., Arnorsson, S., Armannsson, H., 1996. Chemical weathering of basalt in southwest Iceland: effects of runoff, age of rocks and vegetative/glacial cover. Am. J. Sci. 296, 837–907.

Grosbois, C., Négrel, P., Fouillac, C., Grimaud, D., 2000. Dissolved load of the Loire River: chemical and isotopic characterization. Chem. Geol. 170, 179–201.

Goudie, A.S., Viles, H.A., 2012. Weathering and the global carbon cycle: geomorphological perspectives. Earth Sci. Rev. 113, 59–71.

Huh, Y., Edmond, J.M., 1999. The fluvial geochemistry of the rivers of Eastern Siberia: III. Tributaries of the Lena and Anabar draining the basement terrain of the Siberian Craton and the Trans-Baikal Highlands. Geochim. Cosmochim. Acta 63, 967–987.

Han, G., Liu, C.Q., 2004. Water geochemistry controlled by carbonate dissolution: a study of the river waters draining karst-dominated terrain, Guizhou Province, China. Chem. Geol. 204, 1–21.

Han, G., Tang, Y., Xu, Z.F., 2010. Fluvial geochemistry of rivers draining karst terrain in Southwest China. J. Asian Earth Sci. 38, 65–75.

Han, Z.W., Ueda, H., Sakurai, T., 2006. Model study on acidifying wet deposition in East Asia during wintertime. Atmos. Environ. 40, 2360–2373.

Hartmann, J., Jansen, N., Dürr, H.H., Kempe, S., Köhler, P., 2009. Global CO_2 consumption by chemical weathering: what is the contribution of highly active weathering regions? Global Planet. Change 69, 185–194.

Huang, K., Zhuang, G., Xu, C., Wang, Y., Tang, A., 2008. The chemistry of the severe acidic precipitation in Shanghai, China. Atmos. Res. 89, 149–160.

Huh, Y.S., 2003. Chemical weathering and climate – a global experiment: a review. Geosci. J. 7, 277–288.

Karim, A., Veizer, H.E., 2000. Weathering processes in the Indus River Basin: implication from riverine carbon, sulphur, oxygen and strontium isotopes. Chem. Geol. 170, 153–177.

Kump, L.R., Brantley, S.L., Arthur, M.A., 2000. Chemical weathering, atmospheric CO_2 and climate. Ann. Rev. Earth Planet. Sci. 28, 611–667.

Larssen, T., Carmichael, G.R., 2000. Acid rain and acidification in China: the importance of base cation deposition. Environ. Pollut. 110, 89–102.

Larssen, T., Lydersen, E., Tang, D., He, Y., Gao, J., Liu, H., Duan, L., Seip, H.M., 2006. Acid rain in China. Environ. Sci. Technol. 40, 418–425.

Lerman, A., Wu, L., 2006. CO_2 and sulfuric acid controls of weathering and river water composition. J. Geochem. Explor. 88, 427–430.

Lerman, A., Wu, L., Mackenzie, F.T., 2007. CO_2 and H_2SO_4 consumption in weathering and material transport to the ocean, and their role in the global carbon balance. Mar. Chem. 106, 326–350.

Li, S.-L., Calmels, D., Han, G., Gaillardet, J., Liu, C.-Q., 2008. Sulfuric acid as an agent of carbonate weathering constrained by $\delta^{13}C_{DIC}$: examples from Southwest China. Earth Planet. Sci. Lett. 270, 189–199.

Li, S.-L., Chetelat, B., Yue, F., Zhao, Z., Liu, C.-Q., 2014. Chemical weathering processes in the Yalong River draining the eastern Tibetan Plateau, China. J. Asian Earth Sci. 88, 74–84.

Liu, B., Liu, C.-Q., Zhang, G., Zhao, Z.-Q., Li, S.-L., Hu, J., Ding, H., Lang, Y.-C., Li, X.-D., 2013. Chemical weathering under mid- to cool temperate and monsoon-controlled climate: a study on water geochemistry of the Songhuajiang River system, northeast China. Appl. Geochem. 31, 265–278.

Meybeck, M., 2003. Global occurrence of major elements in rivers. In: Drever, J.I. (Ed.), Treatise on Geochemistry, Surface and Ground Water, Weathering, and Soils. Elsevier, pp. 207–223.

Millot, R., Gaillardet, J., Dupré, B., Allègre, C.J., 2002. The global control of silicate weathering rates and the coupling with physical erosion: new insights from rivers of the Canadian Shield. Earth Planet. Sci. Lett. 196, 83–98.

Millot, R., Gaillardet, J., Dupré, B., Allègre, C.J., 2003. Northern latitude chemical weathering rates: clues from the Mackenzie River Basin, Canada. Geochim. Cosmochim. Acta 67, 1305–1329.

Moon, S., Chamberlain, C.P., Hilley, G.E., 2014. New estimates of silicate weathering rates and their uncertainties in global rivers. Geochim. Cosmochim. Acta 134, 257–274.

Moon, S., Huh, Y., Qin, J., van Pho, N., 2007. Chemical weathering in the Hong (Red) River basin: rates of silicate weathering and their controlling factors. Geochim. Cosmochim. Acta 71, 1411–1430.

Moon, S., Huh, Y., Zaitsev, A., 2009. Hydrochemistry of the Amur River: weathering in a Northern Temperate Basin. Aquat. Geochem. 15, 497–527.

Négrel, P., Allègre, C.J., Dupré, B., Lewin, E., 1993. Erosion sources determined by inversion of major and trace element ratios and strontium isotopic ratios in river water: the Congo Basin Case. Earth Planet. Sci. Lett. 120, 59–76.

Noh, H., Huh, Y., Qin, J., Ellis, A., 2009. Chemical weathering in the Three Rivers region of Eastern Tibet. Geochim. Cosmochim. Acta 73, 1857–1877.

Oliva, P., Viers, J., Dupré, B., 2003. Chemical weathering in granitic environments. Chem. Geol. 202, 225–256.

Pacheco, F.A.L., Landim, P.M.B., Szocs, T., 2013. Anthropogenic impacts on mineral weathering: a statistical perspective. Appl. Geochem. 36, 34–48.

Pepin, E., Guyot, J.L., Armijos, E., Bazan, H., Fraizy, P., Moquet, J.S., Noriega, L., Lavado, W., Pombosa, R., Vauchel, P., 2013. Climatic control on eastern Andean denudation rates (Central Cordillera from Ecuador to Bolivia). J. S. Am. Earth Sci. 44, 85–93.

Perrin, A.-S., Probst, A., Probst, J.-L., 2008. Impact of nitrogenous fertilizers on carbonate dissolution in small agricultural catchments: implications for weathering CO_2 uptake at regional and global scales. Geochim. Cosmochim. Acta 72, 3105–3123.

Probst, A., Gh'mari, A.El., Aubert, D., Fritz, B., McNutt, R., 2000. Strontium as a tracer of weathering processes in a silicate catchment polluted by acid atmospheric inputs, Strengbach, France. Chem. Geol. 170, 203–219.

Raymo, M.E., Ruddiman, W.F., 1992. Tectonic forcing of late Cenozoic climate. Nature 359, 117–122.

Raymond, P.A., Cole, J.J., 2003. Increase in the export of alkalinity from North America's largest river. Science 301, 88–91.

Riebe, C.S., Kirchner, J.W., Finkel, R.C., 2003. Erosional and climatic effects on long-term chemical weathering rates in granitic landscapes spanning diverse climate regimes. Earth Planet. Sci. Lett. 224, 547–562.

Roy, S., Gaillardet, J., Allègre, C.J., 1999. Geochemistry of dissolved and suspended loads of the Seine river, France: anthropogenic impact, carbonate and silicate weathering. Geochim. Cosmochim. Acta 63, 1277–1292.

Ryu, J.S., Lee, K.S., Chang, H.W., Shin, H.S., 2008. Chemical weathering of carbonates and silicates in the Han River basin, South Korea. Chem. Geol. 247, 66–80.

Semhi, K., Amiotte Suchet, P., Clauer, N., Probst, J.-L., 2000. Impact of nitrogen fertilizers on the natural weathering-erosion processes and fluvial transport in the Garonne basin. Appl. Geochem. 15 (6), 865–874.

Shin, W.-J., Ryu, J.-S., Park, Y., Lee, K.-S., 2011. Chemical weathering and associated CO_2 consumption in six major river basins, South Korea. Geomorphology 129, 334–341.

Spence, J., Telmer, K., 2005. The role of sulfur in chemical weathering and atmospheric CO_2 fluxes: evidence from major ions, $\delta^{13}C_{DIC}$, and $\delta^{34}S_{SO4}$ in rivers of the Canadian Cordillera. Geochim. Cosmochim. Acta 69, 5441–5458.

Vries, J., Dupré, B., Braun, J.J., Freydier, R., Greenberg, S., Ngoupayou, J.N., Nkamdjou, L.S., 2001. Evidence for non-conservative behavior of chlorine in humid tropical environments. Aquat. Geochem. 7, 127–154.

Vries, W.D., Reinds, G.J., Vel, E., 2003. Intensive monitoring of forest ecosystems in Europe. 2-Atmospheric deposition and its impacts on soil solution chemistry. For. Ecol. Manage. 174, 97–115.

Wang, T.J., Jin, L.S., Li, Z.K., Lam, K.S., 2000. A modeling study on acid rain and recommended emission control strategies in China. Atmos. Environ. 34, 4467–4477.

West, A.J., Galy, A., Bickle, M., 2005. Tectonic and climatic controls on silicate weathering. Earth Planet. Sci. Lett. 235, 211–228.

White, A.F., Blum, A.E., Bullen, T.D., Vivit, D.V., Schulz, M., Fitzpatrich, J., 1999. The effect of temperature on experimental and natural chemical weathering rates of granitoid rocks. Geochim. Cosmochim. Acta 63, 3277–3291.

Wu, W., Zheng, H., Yang, J., Luo, C., Zhou, B., 2013. Chemical weathering, atmospheric CO_2 consumption, and the controlling factors in a subtropical metamorphic-hosted watershed. Chem. Geol. 356, 141–150.

Xu, H., Bi, X.-H., Feng, Y.-C., Lin, F.-M., Jiao, L., Hong, S.-M., Liu, W.-G., Zhang, X.-Y., 2011. Chemical composition of precipitation and its sources in Hangzhou, China. Environ. Monit. Assess. 183, 581–592.

Xu, Y., Wang, C.Y., Zhao, T., 2016. Using detrital zircons from river sands to constrain major tectono-thermal events of the Cathaysia Block, SE China. J. Asian Earth Sci. 124, 1–13.

Xu, Z., Liu, C.-Q., 2007. Chemical weathering in the upper reaches of Xijiang River draining the Yunnan-Guizhou Plateau, Southwest China. Chem. Geol. 239, 83–95.

Xu, Z., Liu, C.-Q., 2010. Water geochemistry of the Xijiang basin rivers, South China: chemical weathering and CO_2 consumption. Appl. Geochem. 25, 1603–1614.

Yoshimura, K., Nakao, S., Noto, M., Inokura, Y., Urata, K., Chen, M., Lin, P.W., 2001. Geochemical and stable isotope studies on natural water in the Taroko Gorge karst area, Taiwan – chemical weathering of carbonate rocks by deep source CO_2 and sulfuric acid. Chem. Geol. 177, 415–430.

Zhang, M., Wang, S., Wu, F., Yuan, X., Zhang, Y., 2007. Chemical compositions of wet precipitation and anthropogenic influences at a developing urban site in southeastern China. Atmos. Res. 84, 311–322.

ZJBGMR: Zhejiang Bureau of Geology and Mineral Resources, 1989. Regional Geology of Zhejiang Province. Geol. Publ. House, Beijing, p. 617 (in Chinese with detailed English abstract).